



Mechanism of thermal decomposition of a pesticide for safety concerns: Case of Mancozeb

N. Giroud^{a,b}, S. Dorge^{a,*}, G. Trouvé^a

^a Laboratoire Gestion des Risques et Environnement, 25, rue de Chemnitz, 68200 Mulhouse, France

^b TREDI, Service Recherche, Technopôle de Nancy-Brabois, 9, avenue de la forêt de Haye, 54505 Vandœuvre-lès-Nancy, France

ARTICLE INFO

Article history:

Received 23 February 2010

Received in revised form 8 June 2010

Accepted 13 July 2010

Available online 22 July 2010

Keywords:

Mancozeb

Dithiocarbamate pesticides

Thermal degradation

Fire incidents

Gaseous and solid pollutants

ABSTRACT

Thermal decomposition under both air and inert atmospheres of a commercial Mancozeb product was investigated through thermogravimetric analysis and laboratory scale thermal treatment from 20 °C to 950 °C, with analysis of gaseous and solid products. The aim of this study is the understanding of the thermal degradation mechanisms of a pesticide under different atmospheres and the chemical identification of the solid and gaseous pollutants which can be emitted during warehouse fires and which can constitute a threat for health and environment. Pyrolysis of Mancozeb takes place between 20 °C and 950 °C and lead essentially to CS₂ and H₂S emissions with formation at 950 °C of MnS and ZnS. Thermal oxidation of Mancozeb under air occurs between 150 °C and 950 °C with formation of CO, CO₂ and sulphur gases (CS₂ and SO₂). The first step (155–226 °C) is the loss of CS₂ and the formation of ethylene thiourea, ZnS and MnS. The metallic sulphides are oxidized in ZnO and MnSO₄ between 226 °C and 650 °C (steps 2 and 3). MnSO₄ is then oxidized in Mn₃O₄ during the last step (step 4) between 650 °C and 950 °C. At 950 °C, carbon recovery is close to 95%. Sulphur recovery is close to 98% with an equal partition between SO₂ and CS₂.

© 2010 Elsevier B.V. All rights reserved.

1. Introduction

Because of the increasing use of pesticides in agriculture and in domestic area during the past 30 years, large amount of these dangerous materials are stored in warehouses before use. Fire is one of the common risks due to storage of dangerous, toxic, and reactive materials. As example, one may remind the incident that occurred in the French city of Beziers during a fire of a stockpile of 88 t of pesticides and its negative environment impact [1]. Indeed, during a warehouse fire, pesticides lead to numerous by-products that may cause disastrous consequences for the environment and the population [2]. However, toxic and eco-toxic effects of a fire are dependent on the materials stored in the warehouse [3]. Studying the thermal decomposition of these molecules is therefore an important way to predict the potential hazard of a pesticide warehouse fire.

Policies nowadays tend to prohibit the use of pesticides in both agriculture and household applications. Europe imposes to ban most of the dangerous molecules [4], whereas objectives are planned to reduce the use of the other pesticides [5]. As a consequence, stockpiles of obsolescent pesticides tend to accumulate in several countries (new EU countries). They also represent an impor-

tant health risk for population in case of fire, water contamination or soil pollution.

Many studies concerning the thermal decomposition of pesticides under various conditions (e.g. temperature and atmosphere) were published in the literature and mainly concern organochlorine pesticides [6,7] and organo-phosphorus pesticides [7–9]. Micro scale experiments of combustion were conducted by Nageswara Rao to characterize and quantify combustion products of several pesticides (monochlorophos, chloropyriphos, butachlor and hexachlorobenzene). Combustion tests were performed at low temperature close to 300 °C in order to simulate chemical fires in warehouses. The analysis of the combustion products by gas chromatography coupled with mass spectrometry indicated the presence of several decomposed organic products of original pesticides in large quantities in the exhaust gas up to 80%. Thermal decomposition of ethyl parathion performed by Andreozzi et al. in a calorimeter led to the same conclusions. Combined effects of the individual components of gaseous organic combustion products may prove to be quite dangerous to life or health of the fire fighters on the site and nearby residents [7,8].

To prevent any pollution, safe destruction of obsolete pesticides has to be carried out [10]. Thermal treatment is mentioned as a method of choice. Kennedy found that thermal treatment at 1000 °C was more likely to degrade most of the pesticides (atrazine, diuron, dieldrine, malathion, zinebe, etc.) than chemical oxidation in solution by hydrogen peroxide, nitric acid, sulphuric acid, sodium

* Corresponding author. Tel.: +33 (0)3 89 32 76 55; fax: +33 (0)3 89 32 76 61.
E-mail address: sophie.dorge@uha.fr (S. Dorge).

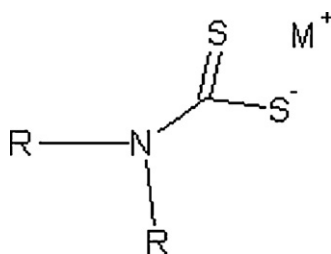


Fig. 1. General structure of dithiocarbamates complexes presented in the literature.

hydroxide or ammonium hydroxide [11]. Pesticides compounds when treated with these solutions exhibited partial decomposition. Results from the incineration of these molecules at high temperature by dry combustion procedure indicated that on the average ten percent of carbon was not accounted for as CO_2 at 900°C [11]. Polychlorobenzenes were very difficult to destroy [12]. Severe conditions are necessary to achieve combustion of polychlorobenzenes leading to carbon dioxide and chlorine in nearly stoichiometric quantities [13]. For example, destruction of hexachlorobenzene may be achieved in the gas phase at 1000°C under 21% of oxygen with 2 s of residence time. At temperatures below 1000°C , concentrations of 35–50% of oxygen in the gas were necessary to complete oxidation of this molecule. Under these conditions, the formation of by-products in the exhaust was minimized [13]. More recently, Karstensen recommended the co-incineration of these products in industrial cement kilns [14]. Cement kiln possess many inherent features which makes it ideal for hazardous waste treatment; high temperatures up to 1500°C , long residence time up to 8 s, surplus of oxygen during and after combustion, good turbulence and mixing conditions, thermal inertia, fixation of trace metals in the clinker, no production of by-products such as slag, ashes and complete recovery of energy and raw materials in the waste. In several countries, several tests demonstrated that the use of hazardous materials containing up to 50% of PCBs as fuel did not change the quality of cement and did not affect emission factors in the exhaust [15–17].

Dithiocarbamates complexes were extensively used in the industry as pesticides, herbicides but also as chelating agent or vulcanization agent. Dithiocarbamates are similar to carbamate groups in which oxygen atoms have been replaced by sulphur atoms. General structure of dithiocarbamates complexes is presented in Fig. 1.

Thermogravimetric analysis (TGA) or differential scanning calorimetry (DSC) techniques often associated with GC–MS analysis were carried out to identify the decomposition products. However, few studies are available concerning dithiocarbamates (DTC) pesticides [18].

Breviglieri studied the thermal decomposition of various dithiocarbamates containing different divalent metallic ions (Cu, Fe, Co, Ni and Zn) by TGA under inert and oxidative atmospheres from room temperature to 1000°C [18] and by DSC. He observed that the thermal stability of DTC under air and nitrogen atmospheres with TG analyser was dependent on the nature of the cation; smaller is the cation, more stable is the molecule. DTC with ions of higher ionic radius as for iron (0.77 nm) decomposes at low temperature (133°C) whereas DTC with the smallest ionic radius as Ni (0.69 nm) starts to decompose at 189°C . Manganese(II) complexes earlier studied in the same experimental conditions followed this behaviour with a decomposition temperature close to 125°C for an ionic radius of 0.80 nm [19].

The thermal behaviour of metal dithiocarbamates complexes has been reviewed by Sengupta in the 1980s. If many results, sometimes contradictory are mentioned because experimental parameters are not all known, main tendencies are pointed out [20]. Data are now available on volatility of metal dithiocarbamates, nature of the metallic ion and R-substitutive groups being

the most important considerations. Among the majority of studied metal dithiocarbamates in inert atmosphere, the common feature observed was that thermal decomposition of metal-DTC proceeded in two steps, the formation of the corresponding metal thiocyanate being the essential step. As for example, decomposition under nitrogen of diethyl Zn-DTC leads to the thiocyanate $\text{Zn}(\text{SCN})_2$ which evolves in the corresponding sulphur (ZnS). The formation of the thiocyanate complex occurs in a relative low temperature range 270 – 370°C . The formation of ZnS by the decomposition of $\text{Zn}(\text{SCN})_2$ is then performed at higher temperature in the range 440 – 670°C . In oxidative atmosphere, Zn-DTC also decomposes in two steps with the formation of metal sulphur ZnS followed by its transformation in metal oxide ZnO. Metal thiocyanate is not formed during thermal decomposition under the presence of oxygen. The presence of oxygen does not significantly affect the temperature ranges of decomposition steps [20].

The thermal behaviour of Maneb, Zineb and Mancozeb (ethylene bis-dithiocarbamate complexes) under nitrogen was studied by Wang using DSC and TGA. IR analyses were used in order to highlight the decomposition mechanism of these products. A four-step decomposition was described but it was not clear whether the tested pesticide was pure or a commercial mixture. Decomposition under inert atmosphere leads to the formation of oxidized minerals whereas the pure materials have not oxygen atom [21]. Four steps mechanisms have been pointed out for both Maneb and Zineb. Concerning Zineb, the first step describes a loss of 1 mol of CS_2 for 1 mol of Zineb with emission of H_2S and COS. This step leads to the formation of ethylene thiourea (ETU), 1 mol of ETU for 2 mol of Zineb, and to an isothiocyanate compound coordinated with zinc. The second step corresponds to the devolatilization of ETU. In the case of Maneb, the first step implies a loss of 1 mol of CS_2 for 2 mole of Maneb. During the second step, another mole of CS_2 , a mole of ETU and a mole of H_2S were also evolved. Two last steps led to the transformation of sulphides to sulphates and then to oxides for both zinc and manganese. The decomposition mechanism of Mancozeb was described by Wang as a combination of Zineb and Maneb degradation. Metallic sulphides were not found in the final solid residues. This fact points out a discrepancy in mechanism of thermal decomposition of metallic-DTC suggested by Wang et al. [21].

In this work, thermal decomposition under air and under inert atmosphere of a commercial Mancozeb product (mainly used as fungicide and herbicide in the EU) was investigated in order to predict nature and concentration of by-products and gases released during a warehouse fire where different atmospheres may be present. The concentrations of emitted gases would allow transport phenomena modelling in ambient air. Experimental parameters were chosen to represent different conditions that may occur during warehouse fires (under inert and air atmospheres and low and high heating rates). Chemical compositions of residues were also characterized to predict solutions for their disposal.

2. Experimental study

2.1. Materials

A commercial Mancozeb based pesticide was used in this study. The active ingredient (Mancozeb–85 wt.%) is composed of zinc ethylene bis-dithiocarbamate (Zineb) and manganese ethylene bis-dithiocarbamate (Maneb) as shown in Fig. 2 [21]. Mancozeb was used as received under powder form.

The active ingredient is formulated with 10 wt.% of calcium lignosulfonic acid salt, 3 wt.% of hexamethylenetetramine (HMTA), 1 wt.% of water and 0.1 wt.% of ethylene thiourea. ETU is one of the decomposition products of Mancozeb.

Elemental composition of the commercial product is given in Table 1. C, H, N, S elements were analysed by the Centre National

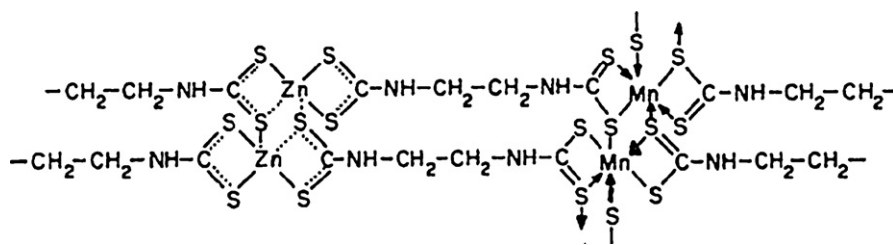


Fig. 2. Chemical structure of Mancozeb proposed by Wang.

Table 1
Elemental composition of Mancozeb (wt.%).

C	H	N	S	Zn	Mn	Ca	O
17.3	2.1	9.4	41.6	2.3	18.1	0.1	9.1

de la Recherche Scientifique (Vernaison, France). Metals as Ca, Mn and Zn were determined by flame atomic absorption spectroscopy. Oxygen amount was determined by difference at 100%.

2.2. Analytical techniques

Experiments were performed using a TG SETARAM Setsys 12 in a 5 μl quartz crucible under a 12 NL h^{-1} of both air and nitrogen flow. A mass of 8–15 mg of product was heated at 5 $^{\circ}\text{C min}^{-1}$ and 20 $^{\circ}\text{C min}^{-1}$ from 20 $^{\circ}\text{C}$ to 950 $^{\circ}\text{C}$. Laboratory scale experiments were carried out in a vertical laboratory furnace. A quartz reactor (diam. 40 mm) and a quartz grid were used. A mass close to of 190 mg of product was heated at 5 $^{\circ}\text{C min}^{-1}$ from room temperature to 950 $^{\circ}\text{C}$ under air or nitrogen flow of 45 NL h^{-1} .

Mole fractions of gases in the exhaust (CO_2 , CO, NO and SO_2) at the reactor and the TG outflows were measured by Infrared analysers Rosemont (BINOS 100 for CO and CO_2 : range 0–10% and 0–20%, respectively; and BINOS 1004 for NO: range 0–1000 ppm) and COSMA CRISTAL 300 (range 0–1%) for SO_2 . Oxygen was quantified by a paramagnetic analyser ARELCO PROA R (range: 0–25%).

Analysis of H_2S , COS, and CS_2 were only performed in the laboratory scale experiment using a gas chromatograph Varian CP-4900. The following parameters were applied: pressure: 150 kPa, gas vector: helium, column: PPQ H BF poraplot Q, column length: 10 m, detector: thermal conductivity detector (TCD), T transfer: 38 $^{\circ}\text{C}$, T injector: 110 $^{\circ}\text{C}$, T column: 150 $^{\circ}\text{C}$, gas flow rate: 0.2–4.0 mL min^{-1} , injection: 100 ms, purge: 10 s, stabilisation: 5 s. Due to long analysis time (87 s) to elute CS_2 ($t_r=81.3$ s), analytical frequency is low (1 analysis every 2 min) and results for CS_2 , COS and H_2S are semi-quantitative.

Results are the average of four experiments for both TGA and in the vertical reactor. Mean relative standard deviation of recovery efficiencies is at least 7%.

The shapes of the curves SO_2 , CO_2 and CO obtained during TGA experiments are similar to those obtained in the laboratory scale device. It reveals the same thermal behaviour of Mancozeb between TG analysis and laboratory scale experiment.

HPLC analysis of ETU in the solid residue was performed after the thermal treatment at 190 $^{\circ}\text{C}$. The extraction of ETU from solid residue was carried out in a solution of methanol 90%–water 10% in ultrasonic bath during 10 min. The solution was then filtered and

analysed by HPLC analysis on a Varian 9012 HPLC system working with an UV detector (Varian 9050). The following conditions were applied: stationary phase: C-18, column length: 220 mm, mobile phase: MeOH–water (10:90), flow rate: 1 mL min^{-1} , pressure: 130–140 atm, T column: 40 $^{\circ}\text{C}$, UV detector (D_2 lamp): 234 nm. The retention time is 4.8 min. The method used is extracted from the OHSAS recommendation for ETU analysis [22].

Infrared spectroscopy was performed on a Bruker IFS 66/S with an MCT detector. Drift method was applied with KBr to record spectra in the range 600–4000 cm^{-1} .

Electron microscopy studies (imaging, selected area electron diffraction (SAED)) were performed with a Philips CM20 microscope with a LaB6 cathode operating at 200 kV. Elemental analyses were carried out by energy dispersive X-ray spectrometry (EDXS) using an EDAX spectrometer. For TEM characterizations, samples were previously dispersed in anhydrous ethanol by sonication during 2–3 min. A drop of the obtained suspension was deposited onto a carbon film supported on a copper grid which was further introduced into the microscope column. TEM characterizations were performed on the residual materials obtained from thermal treatment of Mancozeb at different temperature.

3. Results and discussion

3.1. Pyrolysis of Mancozeb

Experiments were performed under two different heating rates. Table 2 gives the mass losses during these experiments. As shown in Table 2, the influence of the heating rates on mass losses is not significant for each decomposition step. So, mechanism of decomposition was studied at the low heating rate of 5 $^{\circ}\text{C min}^{-1}$ to have the best separation of the decomposition steps. Working at low heating rate favours thermal equilibrium in the sample. Fig. 3 shows TG curve and SO_2 , H_2S and CS_2 emissions during pyrolysis of Mancozeb under inert atmosphere at the heating rate of 5 $^{\circ}\text{C min}^{-1}$. Gaseous emission curves were similar at 20 $^{\circ}\text{C min}^{-1}$. A small mass loss of 1% is observed between 80 $^{\circ}\text{C}$ and 120 $^{\circ}\text{C}$ that is attributed to the evaporation of water contained in Mancozeb. CS_2 emissions were only recorded during the thermal treatment of Mancozeb in the laboratory scale device whereas SO_2 emissions were recorded in both experiments. Laboratory experiments were performed in

Table 2
Mass losses and temperature range of technical Mancozeb during TGA under inert atmosphere.

	Water content	ML 1	ML2	ML3	Residue
Temperature range ($^{\circ}\text{C}$)	80–120	120–200	200–260	260–950	950
Mass losses (%) 5 $^{\circ}\text{C min}^{-1}$	1	27	22	15	Percentage of solid residue = 35
Mass losses (%) 20 $^{\circ}\text{C min}^{-1}$	2	26	27	13	Percentage of solid residue = 32

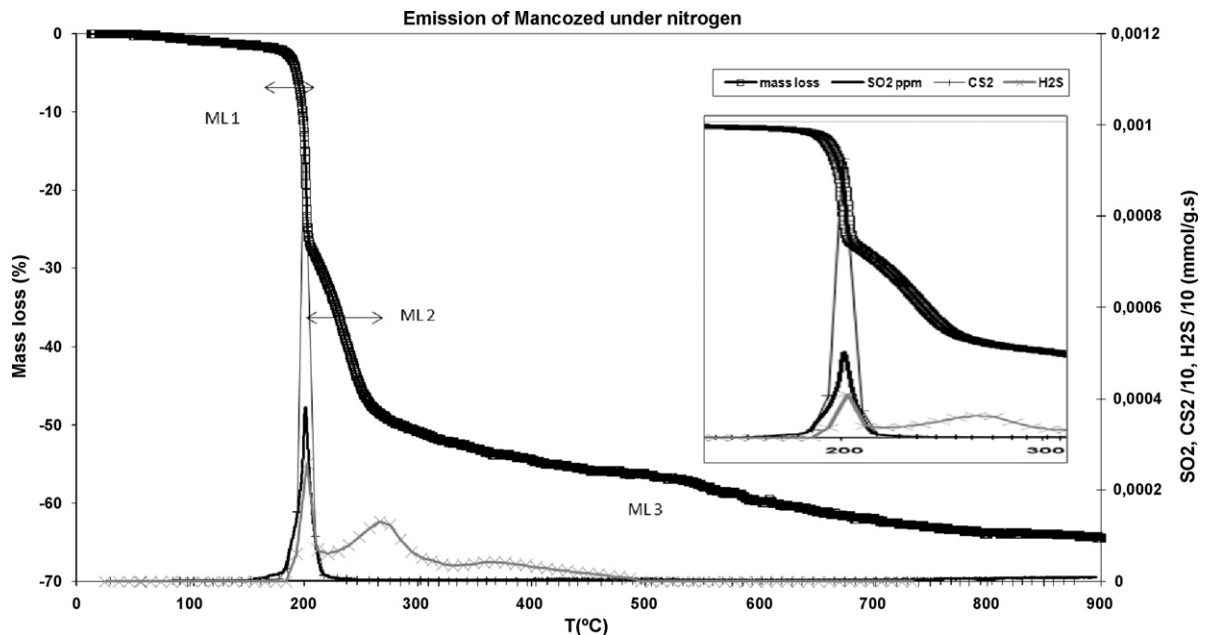


Fig. 3. TG curve and emissions of SO_2 , H_2S and CS_2 per gram of product during pyrolysis of technical Mancozeb (5°C min^{-1}).

the same conditions than those used for TG analysis (same heating rate and atmosphere). The shape of the curve of SO_2 obtained during laboratory scale experiment is totally similar to the one obtained during TG analysis. This result shows an identical thermal behaviour of technical Mancozeb during the experiments at different scale.

Fig. 3 reveals that decomposition of Mancozeb occurs in three main steps with gaseous emissions of SO_2 , H_2S and CS_2 at 200°C . H_2S is also observed until 500°C . This thermal behaviour under nitrogen atmosphere differs from this previously obtained by Wang et al. [21]. He mainly observed an additional mass loss at high temperature between 750°C and 850°C . The amount of emitted SO_2 is low and corresponds to 0.6% of the sulphur present in initial product. CO and CO_2 were also emitted, mainly between 440°C and 950°C . Value for carbon balance sheet was not calculated because amounts of carbon oxides were too low.

First weight loss occurs between 25°C and 200°C . This weight loss of 26.5% is mainly associated with CS_2 and H_2S emissions with few amounts of SO_2 and CO . CS_2 formation was already observed by Wang who suggested the emission of 1 mol of CS_2 per mole of Mancozeb and the formation of ETU during the first step of thermal decomposition of Mancozeb under nitrogen atmosphere [21]. The loss of 1 mol of CS_2 per mole of Mancozeb represents in theory 24 wt.% of the technical product which is consistent with the observed weight loss of 26.5%. The presence of oxygen in initial product can explain the partial oxidation of CS_2 and H_2S in SO_2 . SO_2 emissions were only observed during this step. Water was not emitted during pyrolysis.

The second region between 200°C and 260°C represents 22% of weight loss. H_2S emissions are detected during this decomposition and a thin deposit was observed on the walls of the reactor, in its cold part. Analysis of this deposit by HPLC reveals presence of ETU, formed during the first step of the decomposition of technical Mancozeb. Second mass loss is mainly due to H_2S emissions and devolatilization of ETU followed by its condensation in the cold part of the reactor. IR analysis of the residue at 260°C gives a band at 2065 cm^{-1} which can be attributed to isothiocyanate organic compounds. These compounds coordinated with zinc and manganese species, were already observed by Wang et al. [21].

In this temperature range ($200\text{--}260^\circ\text{C}$), partial decomposition of the calcium lignosulfonic acid salt also occurs. Indeed TG of this pure compound indicates a 30% mass loss at 260°C . It represents only a 3% mass loss in the case of technical Mancozeb where initial content of calcium lignosulfonic acid salt is about 10 wt.%. It corresponds to the primary decomposition of lignocellulosic materials (devolatilization reactions) which generally starts from 200°C to 450°C (as examples, $237\text{--}395^\circ\text{C}$ for wood pellets, $234\text{--}393^\circ\text{C}$ for pine wood, and $178\text{--}384^\circ\text{C}$ for cacao residue). Temperature ranges, pyrolysis rate and yields, depend on various parameters such as properties of the biomaterials (chemical composition, ash content and composition, particle size and shape, mass sample, density, moisture content ...), temperature, pressure and heating rate [23–25].

Between 260°C and 950°C , a continuous weight loss was observed. It corresponds to the secondary reactions of primary tar vapours obtained during both pyrolysis of lignosulfonate salt and Mancozeb residue. At high temperature, the volatile condensable organic products form low-molecular weight gases and char. Lignin is an amorphous polyphenolic constituent able to give high amount of char when heated at high temperature under inert atmosphere [26]. Thermal decomposition of pure lignin by TGA at $10^\circ\text{C min}^{-1}$ under nitrogen atmosphere started at low temperature close to 200°C and led to a mass of char of 43% by weight at 550°C [26]. Secondary reactions are classified as homogeneous and heterogeneous and include processes such as cracking, partial oxidation, re-polymerization and condensation [27]. These reactions generate low-molecular weight gases as CO and CO_2 which can explain the observed emissions of CO and CO_2 from 400°C to 950°C . Thermal analysis of pure calcium lignosulfonic acid salt leads essentially in this temperature range to CO and CO_2 emissions and major part of CO was obtained at high temperature ($600\text{--}900^\circ\text{C}$).

At 950°C , 35% of sample weight is remained. It could correspond very well to the presence of sulphides (ZnS and MnS which represent a percentage of the initial weight of 30.7%). The difference could be attributed to the formation of char from pyrolysis of the calcium lignosulfonic acid salt and Mancozeb residue. These sulphides are produced by transformation of the isothiocyanate organic compounds in metal thiocyanate in the temperature range of $270\text{--}370^\circ\text{C}$. $\text{M}(\text{SCN})_2$ is then decomposed in metal sulphides

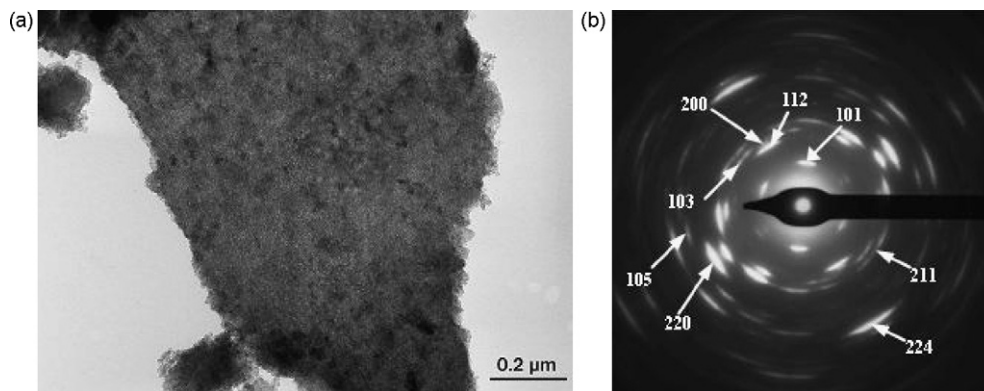


Fig. 4. (a) Bright-field TEM micrograph of Mn_3O_4 particles present in the residue obtained after thermal treatment at 950°C of technical Mancozeb in inert atmosphere and (b) related SAED pattern.

between 440°C and 670°C [20]. TEM/EDXS observations performed on the residue obtained after the thermal treatment at 950°C , confirm the presence of sulphides of manganese and zinc.

Indeed, in some particles, the low content of oxygen (O/S inferior to 0.3) determined by EDXS analysis and the atomic ratio $S/(\text{Mn}+\text{Zn})$ equal to 1 and closed to the theoretical ratio corresponding to MnS and ZnS , indicate the presence of sulphides. Polycrystalline tetragonal Mn_3O_4 phase (space group $I4_1/amd$) was also identified by selected area electronic diffraction (Fig. 4). Several atomic ratios O/Mn of 1, 1.3 and 1.7 were observed by EDXS analyses performed on several particles and reveal the presence of another manganese oxide phases (MnO , Mn_3O_4 , and Mn_2O_3). This result is confirmed by DRX analysis on the residue of the laboratory scale experiment, which indicates the presence of MnS and MnO . The residue is mainly made of a mixture of oxides with MnO as main phase, sulphides and sulphur particles. This result differs from the conclusion of Wang who did not observe sulphide compounds. Wang attributed his last mass loss during the pyrolysis occurring in the temperature range $750\text{--}850^\circ\text{C}$ to the formation of metallic oxides from the corresponding sulphates.

3.2. Thermal degradation of Mancozeb in air atmosphere

Experiments were performed under two heating rates (5°C min^{-1} and $20^\circ\text{C min}^{-1}$). Mass losses were similar at the two heating rates (Table 3). An increase of the heating rate does not modify composition and concentration of emitted species in the exhaust. As discussed above, the 5°C min^{-1} of heating rate was also chosen to solve the mechanism. TG curve and gaseous emissions (SO_2 , CO and CO_2) of thermal degradation of Mancozeb under air atmosphere in TG analysis are plotted in Fig. 5a. Emissions of CS_2 , H_2O and COS (Fig. 5b) were obtained in the laboratory scale device. H_2S is not observed during the thermal treatment of technical Mancozeb in air atmosphere. The shape of the curves of SO_2 , CO and CO_2 is in good agreement with the one obtained for the TG curve.

A first mass loss occurring at 110°C (1 wt.%) corresponds to the drying of the material and generates H_2O emissions (Fig. 5b). Thermal decomposition of technical Mancozeb in air atmosphere starts at 155°C and takes place in four major steps as indicated in Table 3.

First mass loss (29 wt.%) occurs between 155°C and 226°C with formation of gaseous species (SO_2 , CS_2 , COS , H_2O , CO and CO_2). The thermocouple located under the grid records a raise of 20°C corresponding to exothermic reactions. This mass loss is a superposition of three phenomena: The total devolatilization of HMTA which occurs from 150°C to 226°C (3 wt.%). Indeed, TG analysis of this pure compound indicates a 100% mass loss at 226°C and does not generate gaseous emissions. The decomposition of the sulfonic groups from the lignosulfonic acid calcium salt which starts at 150°C and continues during the second mass loss until 410°C . TG analysis of this pure salt shows a weight loss at 216°C equal to 19.1 wt.%. It represents 1.9 wt.% in the first mass loss of technical Mancozeb at this temperature. The first step of the decomposition of Mancozeb itself as mentioned in the safety data sheet (192°C). A sharp peak of CS_2 ($170\text{--}200^\circ\text{C}$) was recorded with a maximum at 201°C . A sharp peak is also observed at 200°C on the SO_2 , COS , CO and CO_2 curves. These gases come from the oxidation of a part of CS_2 . The amount of emitted CS_2 cannot be quantified with the micro-chromatograph due to its low recording frequency. The mass loss observed of 29 wt.% is due to total devolatilization of HMTA (3%) and partial decomposition of calcium lignosulfonic acid salt (1.9%). 24% are missing and correspond to the loss of 1 mol of CS_2 per mole of pure Mancozeb.

A chemical characterization of the solid residue obtained at 190°C after the first mass loss was performed by HPLC and TEM analyses. HPLC analysis reveals the presence of ETU in the residue at 190°C but quantification was not performed. ETU is probably a reaction intermediate formed during the Mancozeb thermal decomposition in air. The TEM characterization indicates the presence of amorphous MnS and ZnS in the solid residue at 190°C by EDXS analyses on several particles which show a ratio $S/(\text{Zn}+\text{Mn})$ between 1 and 1.7 and a low oxygen content (Fig. 6a). At 190°C , the decomposition of Mancozeb in air leads to the loss of CS_2 and the formation of ETU and amorphous sulphides of manganese and zinc. Crystalline phase was not observed by SAED meaning that particles in the residue at this temperature were amorphous. For particles having a ratio $S/(\text{Zn}+\text{Mn})$ higher than 1, the excess of sulphur in comparison to the stoichiometry may be attributed to organic sulphur compounds (ETU and calcium lignosulfonic acid salt) which are practically not decomposed at this temperature. Indeed, TG analysis of pure ETU in air atmosphere indicates a devolatilization

Table 3
Mass losses and temperature range of technical Mancozeb during thermogravimetric analysis under air atmosphere (5°C min^{-1}).

	Water content	ML 1	ML2	ML3	ML4	Residue
Temperature range ($^\circ\text{C}$)	80–120	155–226	226–410	410–650	650–950	950
Mass losses (%) 5°C min^{-1}	1	29	10	17	11	Percentage of solid residue = 32
Mass losses (%) $20^\circ\text{C min}^{-1}$	2	31	9	17	10	Percentage of solid residue = 31

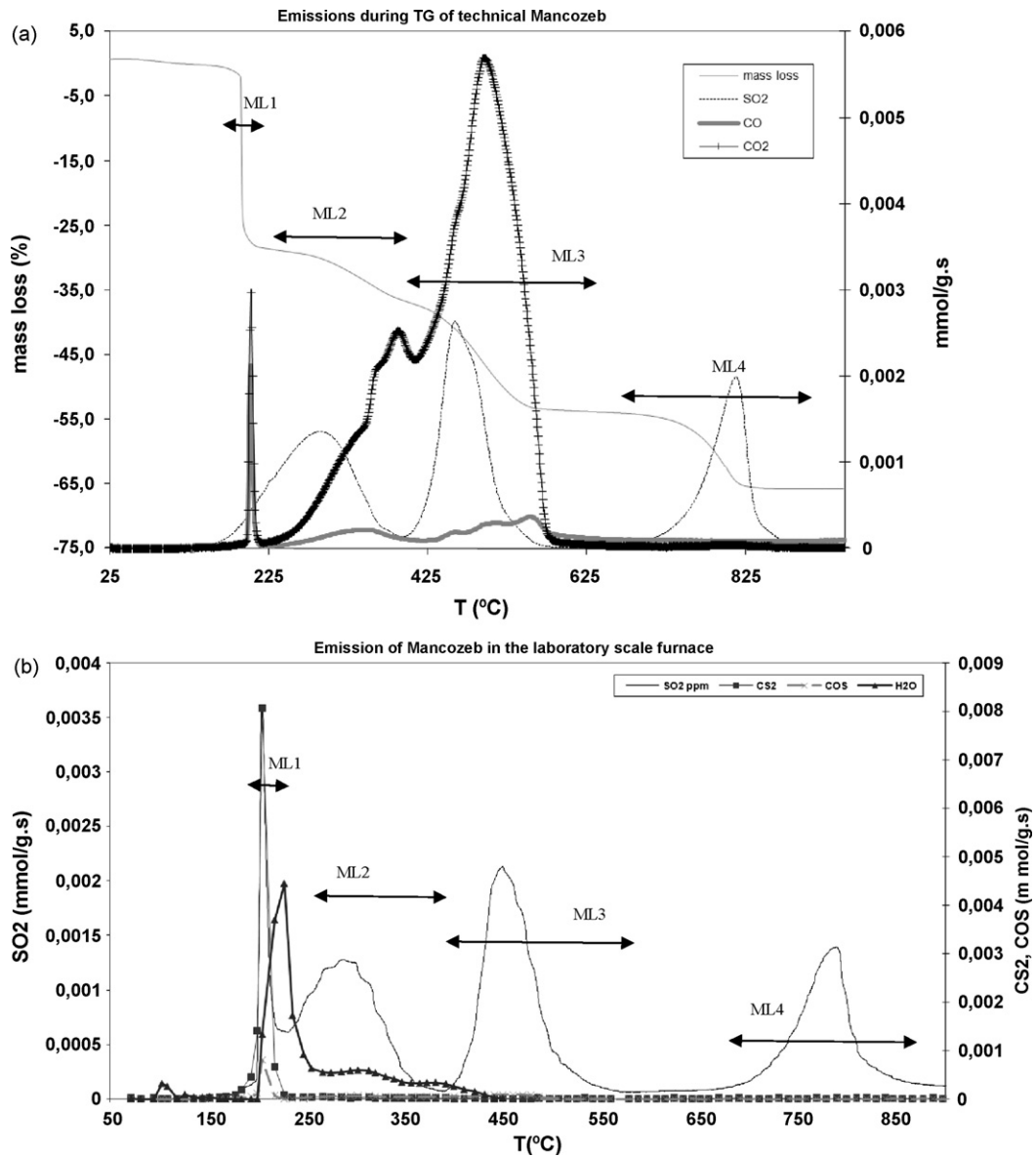


Fig. 5. (a) SO_2 , CO and CO_2 emissions during thermogravimetric analysis of technical Mancozeb (12 NL h^{-1} air flow rate, $5^{\circ}\text{C min}^{-1}$). (b) SO_2 , CS_2 , COS and H_2O (arbitrary unit) emissions during thermal treatment of technical Mancozeb in laboratory scale experiment (45 NL h^{-1} air flow rate, $5^{\circ}\text{C min}^{-1}$).

of ETU at only 220°C and TGA of the pure calcium lignosulfonic acid salt only shows 12% mass loss at 190°C . Oxygen observed in EDXS analyses comes from organic compounds. The possible formation of manganese and zinc oxides at this step, could also explain the presence of oxygen in EDXS quantifications.

The two following mass losses (ML2 and ML3) occurring between 226°C and 650°C correspond to the total decomposition of the calcium lignosulfonic acid salt in calcium carbonate which was observed by TEM (EDXS analyses) in the solid residue of the thermal treatment of pure lignosulfonic acid salt at 900°C in air. TG analysis of this pure compound as shown in Fig. 7 (TG and SO_2 , CO_2 and CO emissions) under air, indicates a final mass loss equal to 85% and only one peak of SO_2 between 150°C and 450°C with a maximum at 290°C which corresponds to the loss of the sulfonic groups. This emission appears during decomposition of technical Mancozeb (Fig. 5a) in the first peak of SO_2 between 150°C and 410°C . Decomposition of pure lignosulfonic acid salt also shows three distinct major peaks of CO and CO_2 (the major species) at 330°C , 470°C and 580°C with a minor peak at 710°C . The first peak of CO and CO_2 at 330°C could correspond to the devolatilization of

cellulosic polymers present in the lignosulfonic acid salt according to literature data [28]. The maximal peak at 470°C is due to the decomposition of lignin which starts at 410°C and is achieved at 520°C . CO and CO_2 emissions during the third step between 520°C and 600°C correspond to the combustion of the residual char as for lignocellulosic materials [29,30]. These three phenomena appear in Fig. 5a as more or less pronounced "shoulders" at 350°C , 470°C and 550°C on the CO and CO_2 emissions curves.

In this temperature range, between 226°C and 650°C , carbon reaction intermediates formed during Mancozeb decomposition itself (ETU and unidentified organic sulphur compounds) are also oxidized, leading to the formation of SO_2 and carbon oxides, mainly CO_2 (ratio CO/CO_2 equal to 0.1). Two distinct peaks of SO_2 are observed during thermal treatment of technical Mancozeb in air atmosphere between 220°C and 580°C . The first peak of SO_2 with a maximum at 290°C is attributed to the loss of the sulfonic groups of the lignosulfonic salt and to the decomposition of the sulphur reaction intermediates formed during the first step of the decomposition of Mancozeb itself. It represents 16% of the sulphur present in initial technical product (Table 4). TG analysis of pure ETU in

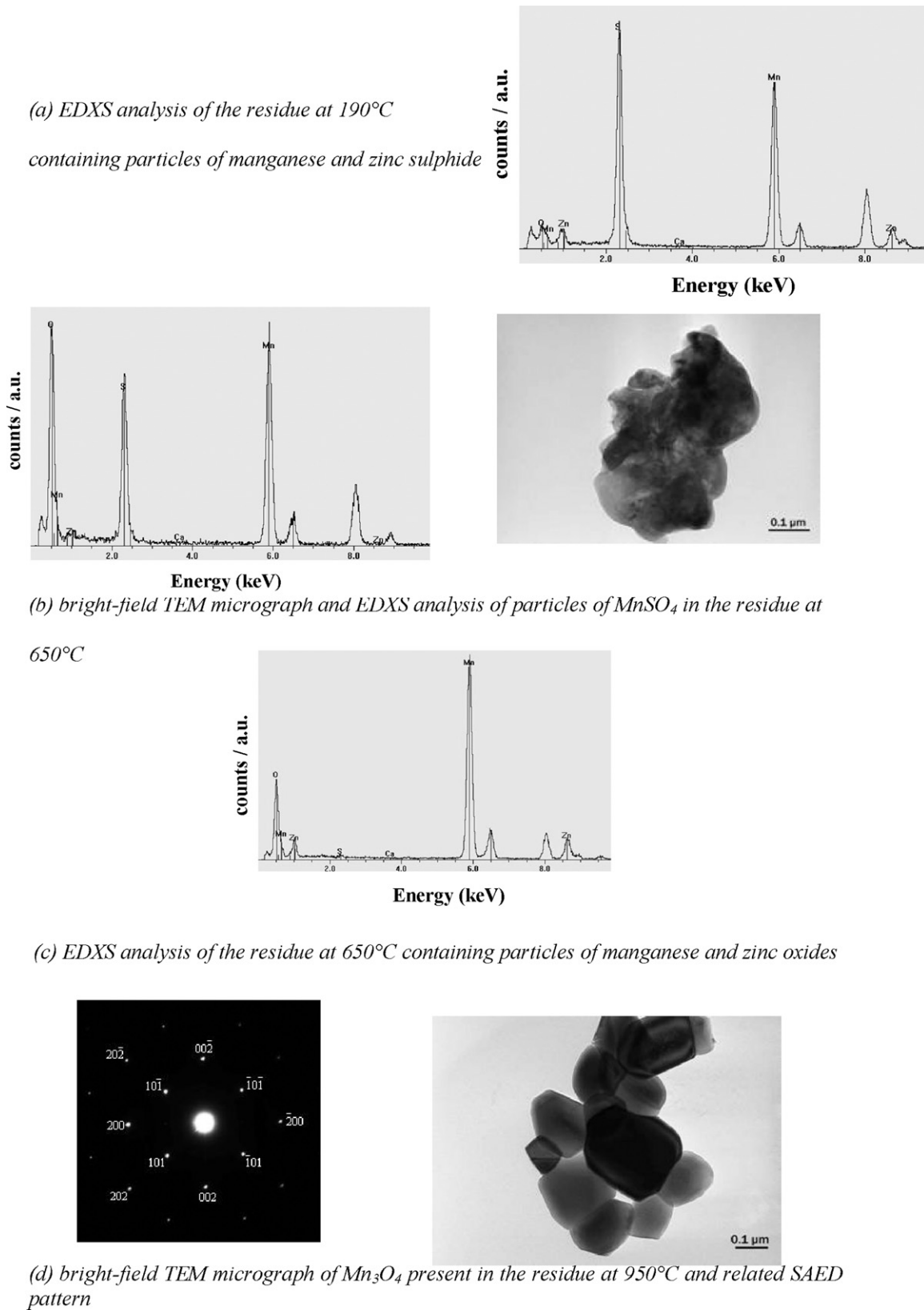


Fig. 6. Results of TEM analyses (EDXS analyses and SAED pattern) of the residue of the thermal treatment of technical Mancozeb at different temperatures.

air atmosphere reveals that ETU is not decomposed but simply devolatilized and then condensed in the cold part of the reactor, without SO_2 emissions. The SO_2 peak observed between 220 °C and 400 °C during thermal treatment of technical Mancozeb in air atmo-

sphere does not come from ETU decomposition but comes from sulphur organic intermediate compounds degradation.

The third peak of SO_2 between 400 °C and 600 °C with a maximum at 460 °C, can be generated by the decomposition of

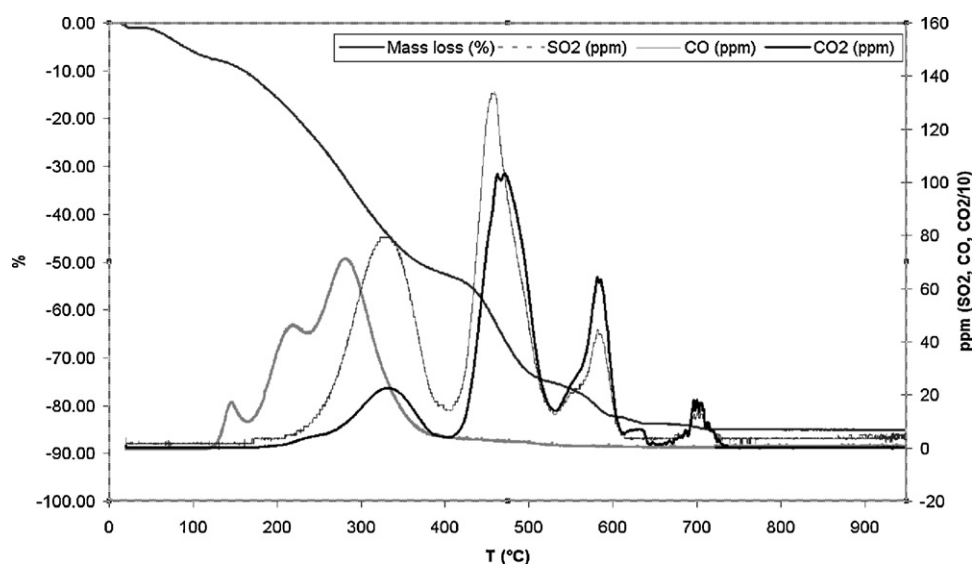


Fig. 7. TG of calcium lignosulfonic acid salt under air (12 NLh^{-1} , 5°C min^{-1}) with SO_2 , CO and CO_2 emissions.

manganese and zinc amorphous sulphides formed during the first step, in both manganese sulphate and oxides and in zinc oxide ZnO , respectively (all these phases were observed on solid residues obtained at 650°C by TEM/EDXS analyses as seen in Fig. 6b and c). Indeed, TG experiment of pure ZnS in air atmosphere shows a total decomposition of this product in ZnO and SO_2 from 550°C to 650°C with a sulphur balance sheet equal to 100%. Thermal degradation of MnS in air atmosphere occurs in two steps. The first stage is the simultaneous formation of orthorhombic MnSO_4 (space group: $Cmcm$) and tetragonal Mn_3O_4 (space group: $I4_1/amd$) from 290°C to 510°C with formation of SO_2 emissions. These two phases were identified by TEM analysis (EDXS and SAED) on the residue of pure MnS heated at 650°C . Between 670°C and 850°C , MnSO_4 is then decomposed in tetragonal Mn_3O_4 with SO_2 emissions (100% of sulphur of initial MnS is emitted as SO_2). This reaction corresponds to the last mass loss of decomposition of technical Mancozeb (Fig. 5a) leading to the last emission of SO_2 between 670°C and 900°C .

The sum of moles of SO_2 per gram of technical Mancozeb emitted during the two last mass losses (ML3 and ML4, as shown in Table 4) is equal to the sum of elemental moles of Mn and Zn contained in one gram of technical Mancozeb. This result strengthens the hypothesis that metallic sulphides are totally oxidized during the two last steps. Quantity of SO_2 emitted during ML4 strictly corresponds to the observed mass loss that characterizes the transformation of MnSO_4 in Mn_3O_4 . Crystalline phase of this manganese oxide was detected by TEM on the residue at 950°C . Indeed the related SAED pattern insert of Fig. 6d displayed in the $[010]$ zone axis diffraction spots characteristic of the tetragonal structure of Mn_3O_4 (space group: $I4_1/amd$).

In Table 4, carbon and sulphur balance sheets are also given under their gaseous species. As shown in Fig. 5b, CS_2 and COS are

emitted in the exhaust, but they were not quantified with enough accuracy.

Under the speciation SO_2 , sulphur balance sheet is equal to 48.4%. During ML1, 1 mol of CS_2 per mole of Mancozeb is emitted which represents 50% of the sulphur contained in Mancozeb. This leads to a total sulphur balance sheet of 98.4%. This balance must be decreased of the amount of SO_2 (4.3% sharp peak ML1) coming from the partial oxidation of CS_2 . Calculated global sulphur balance sheet is then of 94.1%. The same consideration may be added for carbon balance sheet. Emissions of CS_2 represent 18.5% of the carbon of technical Mancozeb. Under carbon oxides (CO and CO_2), total carbon balance sheet is equal to 76.6%. This value corresponds to the sum of carbon present in both forms (as seen in Table 4). This leads to a total carbon balance sheet of 95.1%. This balance must be decreased of the respective amounts of CO and CO_2 (2.7% sharp peak ML1) coming from the partial oxidation of CS_2 . This leads to a total carbon balance sheet of 92.4% during the thermal oxidation of technical Mancozeb by TGA.

3.3. Comparison of the behaviour of Mancozeb under inert and air atmospheres

The first step (ML1) of the Mancozeb decomposition (about 28% mass loss under air and nitrogen) occurs between 120°C and 200°C in both atmospheres and corresponds to the decomposition of the dithiocarbamate group leading to the emission of the gaseous pollutant CS_2 (1 mol of CS_2 per mole of Mancozeb) and the formation of metallic sulphides. Under air, part of the emitted CS_2 is oxidized and generates other pollutants like SO_2 , CO and CO_2 . During nitrogen experiments, only H_2S is well detected in addition to CS_2 . The organic Mancozeb residue remaining after ML1 mainly con-

Table 4

Total amounts of SO_2 , CO and CO_2 emitted during thermal treatment of Mancozeb under air atmosphere during thermogravimetric experiment (5°C min^{-1}).

Mass loss	Total amount (mmol g^{-1} technical Mancozeb)			Molar carbon and sulphur balance sheet (referred to initial technical product) (%)		
	SO_2 (%)	CO_2 (%)	CO (%)	SO_2 (%)	CO (%)	CO_2 (%)
ML1 150–226 °C	0.30	0.24	0.15	2.4	1.7	1.0
ML1 sharp peak	0.56			4.3		
ML2 226–410 °C	1.73	2.65	0.28	13.4	18.4	1.9
ML3 410–650 °C	2.12	7.02	0.70	16.4	48.7	4.9
ML4 650–950 °C	1.54	N/A	N/A	11.9	N/A	N/A
Total	6.25	9.91	1.13	48.4	68.8	7.8

tains ETU in air experiments whereas under nitrogen atmosphere, isothiocyanate intermediates are formed.

Under air atmosphere, the decomposition of the organic Mancozeb intermediates and the calcium lignosulfonate additive which occurs between 200 °C and 600 °C (ML2 and ML3) generates CO and CO₂ emissions in this temperature range, due to the presence of oxygen in the gas phase. SO₂ emissions are also observed during these steps (ML2 and ML3) under air and results from the decomposition of the lignosulfonate salt and the oxidation of the metallic sulphides in oxides (ZnO and Mn₃O₄) and manganese sulphate MnSO₄. The transformation of MnSO₄ in Mn₃O₄ at high temperature (800 °C) also generates SO₂ emissions. At 900 °C, the final residue after thermal treatment under air is composed of manganese and zinc oxide and represents a mass of 32 wt.%. In nitrogen experiments, only H₂S is emitted between 200 °C and 900 °C and the solid residues obtained at 900 °C (35 wt.%) are metallic sulphides (ZnS and MnS) and oxides whereas in air, these compounds are totally oxidized between 400 °C and 850 °C.

4. Conclusions

Stockpiles of obsolete pesticides constitute a threat for health and environment. Chemical fires seem to be one of the most important hazards. Prediction of by-products and gases released during warehouse fires is a major point of view to plan safety actions. Warehouse fires generate solid wastes that contain pollutants. Chemical identification of these pollutants is necessary to predict solutions for their disposal.

The active ingredient (Mancozeb—85 wt.%) was composed of zinc ethylene bis-dithiocarbamate (Zineb) and manganese ethylene bis-dithiocarbamate (Maneb). Additives were also present as calcium lignosulfonic acid, HMTA, water and traces of ETU. Mechanisms were determined by the analysis of gaseous species evolved during the thermal treatment and by chemical characterization of solid residues. Behaviours of individual components were taken into account in the same experimental conditions in order to highlight possible interactions of these components in the available product.

Thermal degradation of technical Mancozeb takes place in large temperature range between 20 °C and 950 °C in both atmospheres. The molecule of Mancozeb and calcium lignosulfonic acid is both decomposed in inert atmosphere leading mainly to the gaseous emissions of CS₂ and H₂S. Low amounts of carbon oxides are evolved during the decomposition of the calcium lignosulfonic acid. The lignocellulosic part of this additive reacts as wood polymers. Solid residues are composed of Mn and Zn sulphides at 950 °C. An increase of the heating rate from 5 °C min⁻¹ to 20 °C min⁻¹ does not modify the thermal behaviour of Mancozeb under nitrogen atmosphere.

Thermal oxidation of the technical Mancozeb under air proceeds in four main steps between 150 °C and 950 °C. The first step of the decomposition of the technical product occurs between 155 °C and 226 °C and corresponds to the loss of 1 mol of CS₂ per mole of Mancozeb with the formation of manganese and zinc sulphides and ETU. The two following mass losses occurring between 226 °C and 650 °C correspond to the total decomposition of the calcium lignosulfonic acid salt in calcium carbonate generated in the exhaust carbon oxides and sulphur dioxide. Oxidation of metallic sulphides also takes place at this temperature range, mainly during the third mass loss with emission of SO₂. ZnS forms ZnO whereas MnS gives manganese oxides and the sulphate MnSO₄ as an intermediate mineral. MnSO₄ is then oxidized in Mn₃O₄ during the last step (fourth mass loss) between 650 °C and 950 °C with the formation of SO₂ in the exhaust. At 950 °C, carbon recovery in both forms CO and CO₂ is close to 95%. Sulphur recovery is close to 98% with an equal par-

tion between SO₂ and CS₂. At the final temperature, metals are oxidized under the speciation of ZnO and Mn₃O₄, respectively. As observed during pyrolysis, the influence of the heating rate is also not significant in presence of oxygen.

Specific gases are observed for both atmospheres: CS₂, H₂S under nitrogen and SO₂, CS₂, carbon oxides under air, respectively. If under nitrogen atmosphere, manganese and zinc sulphides are present in the solid residue at the final temperature, the composition of the residues under air varies with the temperature. Metallic sulphides, sulphates and oxides are observed depending on the temperature.

Because of the chemical structure of dithiocarbamate molecules, any of these pesticides compounds would generate the same type of pollutants during thermal degradation in warehouse fires, particularly sulphur gaseous products (SO₂, CS₂ and H₂S). This study would be useful for risk assessment during storage fire incidents. These emission data could be introduced in transport phenomena modelling codes to predict dispersion of pollutants in the atmosphere.

References

- [1] Ministère chargé de l'environnement DPPR/SEI/BARPI, Incendie dans un dépôt de pesticides le 27 juin 2005, Béziers, France, No. 30269.
- [2] D.A. Kefalas, M.N. Christolis, Z. Nivolianitou, N.C. Markatos, Consequence analysis of an open fire incident in a pesticide storage plant, *J. Loss Prevent. Proc. Ind.* 19 (2006) 78–88.
- [3] O. Senneca, F. Scherillo, A. Nunziata, Thermal degradation of pesticides under oxidative conditions, *J. Anal. Appl. Pyrol.* 80 (2007) 61–76.
- [4] Directive 1991/689/EC of the European Parliament and of the Council of 12 December, 1991 on Hazardous Wastes, Official Journal of the European Communities No. L 377 of 31 December, 1991.
- [5] Plan Ecophyto 2018 de Réduction des Usages de Pesticides 2008–2018. Available from http://agriculture.gouv.fr/sections/magazine/focus/phyto-2018-plan-pour/ecophyto-2018-plan-pour6154/downloadFile/FichierAttache_5_f0/PLAN_ECOPHYTO_2018.pdf?nocache=1240504850.07 (accessed February, 2010).
- [6] J. Łubkowski, T. Janiak, J. Czermiński, J. Bła- ejowski, Thermoanalytical investigations of some chloro-organic pesticides and related compounds, *Thermochim. Acta* 155 (1989) 7–28.
- [7] R. Nageswara Rao, S. Khalid, T. Rajani, S. Husain, Gas chromatographic–mass spectrometric separation and identification of combustion products of organophosphorus and chlorine pesticides and evaluation of their impact on the environment, *J. Chromatogr. A* 954 (1–2) (2002) 227–234.
- [8] R. Andreozzi, G. Ialongo, R. Marotta, R. Sanichirico, Thermal decomposition of ethyl parathion, *J. Loss Prevent. Proc. Ind.* 12 (1999) 315–319.
- [9] R. Kakko, V. Christiansen, E. Mikkola, R. Kallonen, L. Smith-Hansen, K.H. Jørgensen, Toxic combustion products of three pesticides, *J. Loss Prevent Proc. Ind.* 8 (1995) 127–132.
- [10] J. Vijgen, C. Egenhofer, Obsolete (lethal) pesticides, a ticking time bomb and why we have to act now, Tauw Group BV, The Netherlands, 2009, ISBN-13: 978-90-76098-10-4.
- [11] M.V. Kennedy, B.J. Stojanovic, F.L. Shuman Jr., Chemical and thermal methods for disposal of pesticides, *Residue Rev.* 29 (1969) 89–104.
- [12] B. Dellinger, D.L. Hall, W.A. Rubey, J.L. Torres, R.A. Carnes, EPA Research Division, *Revue EPA* (1984)/600/9-84/0-15, 65.
- [13] J. Bonnet, N. El Mejdoub, G. Trouvé, L. Delfosse, Study of the gas phase combustion of hexachlorobenzene, influence of oxygen concentration. Attempt at a global kinetic formulation, *J. Anal. Appl. Pyrol.* 44 (1997) 1–11.
- [14] K.H. Karstensen, N.K. Kinh, L.B. Thang, P.H. Viet, N.D. Tuan, D.T. Toi, N.H. Hung, T.M. Quan, L.D. Hanh, D.H. Thang, Environmentally sound destruction of obsolete pesticides in developing countries using cement kilns, *Environ. Sci. Policy* 9 (2006) 577–586.
- [15] K.H. Karstensen, Burning of Hazardous wastes as co-fuel in a cement kiln—does it affect the environmental quality of cement?—leaching from cement based materials, *Studies in Environmental Science: Environmental Aspects of Construction with Waste Materials*, The Netherlands, 1994, ISBN 0-444-81853-7, pp. 433–451.
- [16] J.F. Chadbourne, Cement kilns, in: H.M. Freeman (Ed.), *Standard Handbook of Hazardous Waste Treatment and Disposal*, McGraw-Hill, 1997, ISBN 0-07-022044-1.
- [17] L.P. Mac Donald, D.J. Skinner, F.J. Hopton, G.H. Thomas, Burning waste chlorinated hydrocarbons in a cement kiln, Environment Canada, Report EPS 4/WP/77-2, 1977.
- [18] S.T. Breviglieri, E.T.G. Cavalheiro, G.O. Chierice, Correlation between ionic radius and thermal decomposition of Fe(II), Co(II), Ni(II), Cu(II) and Zn(II) diethanoldithiocarbamates, *Thermochim. Acta* 356 (2000) 79–84.
- [19] E.T.G. Cavalheiro, M. Ionashiro, G. Marino, S.T. Breviglieri, G.O. Chierice, Correlation between i.r. spectra and thermal decomposition of cobalt(II),

- nickel(II), copper(II) and mercury(II) complexes with piperidinedithiocarbamate and pyrrolidinedithiocarbamate, *Trans. Met. Chem.* 25 (2000) 69–72.
- [20] S.K. Sengupta, Thermal studies on metal dithiocarbamatocomplexes. A review, *Thermochim. Acta* 72 (1984) 349–361.
- [21] G.J. Wang, C.M. Yin, Y. Wang, Y.H. Kong, G.H. Wang, C.Y. Wu, L.F. Zhang, Z.R. Liu, The thermal behaviour of the ethylenebis-dithiocarbamates Maneb, Zineb and Mancozeb. Part 1. The mechanism of the thermal decomposition, *Thermochim. Acta* 220 (1993) 213–227.
- [22] OSHA, Sampling and Analytical Methods/Ethylene Thiourea. Available from <http://www.osha.gov/dts/sltc/methods/organic/org095/org095.html> (accessed January, 2010).
- [23] C. Di Blasi, Modelling chemical and physical processes of wood and biomass pyrolysis, *Prog. Energy Combust. Sci.* 34 (2008) 47–90.
- [24] S. Völker, T. Rieckmann, Thermokinetic investigation of cellulose pyrolysis—impact of initial and final mass on kinetic results, *J. Anal. Appl. Pyrol.* 62 (2002) 165–177.
- [25] E. Biagini, L. Tognotti, Comparison of devolatilization/char oxidation and direct oxidation of solid fuels at low heating rate, *Energy Fuels* 2 (2006) 986–992.
- [26] M. Canetti, F. Bertini, A. De Chirico, G. Audisio, Thermal degradation behaviour of isotactic polypropylene blended with lignin, *Polym. Degrad. Stab.* 91 (2006) 494–498.
- [27] P. Morf, P. Hasler, T. Nussbaumer, Mechanisms and kinetics of homogeneous secondary reactions of tar from continuous pyrolysis of wood chips, *Fuel* 81 (2002) 843–853.
- [28] J.J.M. Órfao, F.J.A. Antunes, J.L. Figueiredo, Pyrolysis kinetics of lignocellulosic materials—three independent reaction model, *Fuel* 78 (1999) 349–358.
- [29] M. Muller-Hagerdorn, H. Bockhorn, L. Krebs, U. Muller, Investigation of thermal degradation of three wood species as initial steps in combustion of biomass, *Proc. Combust. Inst.* 29 (2002) 399–406.
- [30] A. Chouchene, M. Jeguirim, B. Khiari, F. Zagrouba, G. Trouvé, Thermal degradation of olive solid waste: influence of the particle size and oxygen concentration, *Resour. Conserv. Recycl.* 54 (2010) 271–277.